Wideband SIW Based Frequency Selective Surface using Exponential Tapering Technique

Vinayak Mahadik, Jogesh Chandra Dash, *Member, IEEE,* Raju Malleboina, *Student Member, IEEE,*, Shilpa Kharche, Debdeep Sarkar, *Member, IEEE,*

Abstract—In this paper, a new design approach is proposed for a frequency selective surface (FSS) based on surface integrated waveguide (SIW) technique using exponential tapering. Here, the unit cell of the FSS is an exponentially tapered cross-slot structure designed on either side of a low-loss substrate. The FSS exhibits good angular stability for TE and TM polarizations up to 30^0. The FSS element shows $\approx 34\%$ wide bandpass response in the X-band region i.e., -3 dB transmission bandwidth from 8.69 GHz to 12.07 GHz, with low insertion loss of 0.1 dB and sharp roll-off characteristics. Extensive studies on various design parameters such as exponential tapering factor and via dimensions are performed using HFSS full-wave EM solver. To validate the proposed FSS design, a low-cost FR4 substrate is used for fabrication, and the measured results are compared to the corresponding simulation results.

Index Terms—Frequency Selective Surface (FSS), Substrate-Integrated Waveguide (SIW), Exponential Taper.

I. INTRODUCTION

THE Frequency-selective surfaces (FSSs) are planar structures that can filter electromagnetic waves according to their frequency, polarization, and angle of incidence [1]. FSSs have various applications in communication systems, radars, antennas, and shielding devices [2]- [8]. However, conventional FSSs have some limitations, such as narrow bandwidth, high insertion loss, and poor angular stability [3].

To overcome these drawbacks, substrate-integrated waveguide (SIW) based FSSs have been proposed in recent years [4]. SIW is a low-cost and low-loss transmission line that can be easily integrated with planar circuits [5].The SIW based FSSs can achieve wide bandwidth, low insertion loss, and high angular stability by exploiting the waveguide mode propagation and the resonance of the SIW cavities [3]- [6]. Additionally, SIW FSS structures can provide superior filtering characteristics, wider pass-bands, lower cross-talk, improve the Radar cross section (RCS), and provide very good transmission efficiency [7]- [8]. Notably, more applications of SIW based FSS are seen in band-pass filters and slotted array antennas for satellite communication, band-specific communication bands and to address the challenges in streamlining airborne radomes

Vinayak Mahadik and Shilpa Kharche are with the Department of Electronics and Communication Engineering, Terna Engineering College,Mumbai, 400706, India (e-mail: vinayak.mahadik@gmail.com, shilpakharche@ternaengg.ac.in). J.C Dash is with the Department of Electronics and Communication Engineering, NIT, Rourkela, Odisha, 769008, India (email: jcdash92@gmail.com). Raju Malleboina and D. Sarkar are with the Department of Electronics and Communication Engineering, IISc Bangalore 560012, India (email: malleboinar@iisc.ac.in, debdeep@iisc.ac.in)
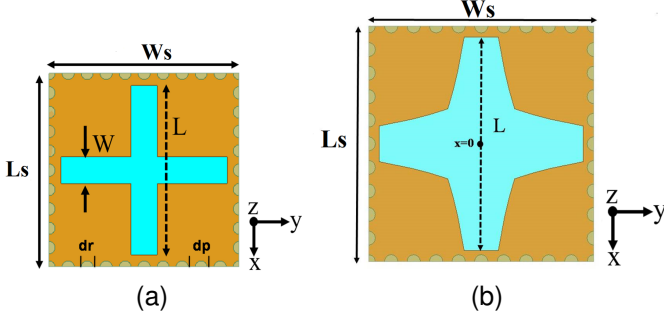
[11]- [15]. The SIW-based FSS is playing a vital role in the deployment of microwave technology in its applications. However, efficient and effective model development is crucial to predict the desired band characteristics for a wide range of configurations [9]. Furthermore, looking at the versatile nature of the SIW based FSS in various applications such as conformality, [10] performance implications can be assessed in air borne applications.

The literature extensively explores Frequency Selective Surfaces (FSS) in the context of radomes, shedding light on diverse structural designs. These designs encompasses both slot-based and patch-based configurations, which exhibits a variety of shapes tailored for specific radome applications.

The utilization of a wideband frequency-selective surface (FSS) [17] featuring a sharp roll-off characteristic and a mushroom-like cavity equipped with four L-shaped slots highlights the significant role of substrate-integrated waveguide (SIW) technology in achieving a 55.8% reduction in unit cell size. This miniaturization, facilitated by SIW's compact planar nature, paves the way for innovative applications in areas demanding size-constrained microwave devices. However, Fabricating structures with precise geometries, such as mushroom-like cavities, can be challenging and may require advanced manufacturing techniques such as photolithography or electron beam lithography. This complexity could increase the fabrication cost and limit scalability.In [18] Y-shaped SIW FSS for stable polarization, this work proposes a novel design that not only maintains polarization stability but also leads to significant advancements in resonance stability and roll-off characteristics.In [19], A meta-surface unit cell is adopted to suppress the grating lobe and achieve miniaturization.It also underscores the importance of the multilayer structures for high angular stability and keenly points out the cost-effectiveness. The structure is a traditional cross slot which is modified further. [20] discusses a design or study related to selective surfaces in the context of antennas and propagation, focusing on achieving a quasi-elliptic bandpass response with a high roll-off frequency.filter's frequency response resembles that of an elliptic filter, which typically exhibits steep roll-off characteristics in the transition between passband and stopband. Importantly, upon analyzing the above structures on performance metrics, it can be conferred that the modeling could be very specifically done to achieve compactness, low profile, miniaturization, and advancement in materials for various design consideration. [21]- [25].

Given the above, this study focuses on the development of an SIW-based Frequency Selective Surface (FSS) employing

Fig. 1. SIW-based FSS unit cell: (a) Design stage 1: Conventional cross slot, and (b) Design stage 2: Exponentially tapered Cross Slot.
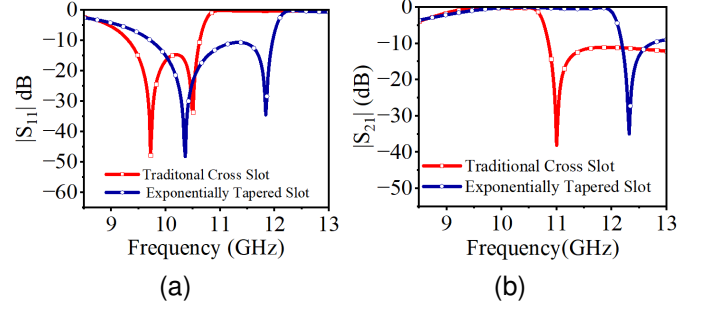

Fig. 2. S-parameters of exponentially tapered cross slot SIW based FSS unit cell in comparison with the traditional (a) Reflection coefficient Vs frequency, and (b) Transmission coefficient Vs frequency.

exponential tapering for wide-band applications. The proposed design aims to harness the benefits of SIW technology and FSS configurations to achieve not only a broad operating bandwidth but also a sharp transition response. The objective is to provide a novel solution that can be instrumental in wide-ranging applications that require wide-band consideration.

In this paper, the exponential tapering shape along with its design theory and detailed analysis for slot type FSS have been studied. A detailed analysis of the variations in the exponential tapering parameter α and its effect on the performance of the FSS is presented herein.

II. DESIGN PROCEDURE OF PROPOSED EXPONENTIAL TAPER FSS

To provide a better understanding of the proposed exponentially tapering FSS slot design, a two-stage design process is provided as shown in Fig. 1. Initially, in stage 1, a traditional cross-slot-shaped SIW-based FSS unit cell design is provided in Fig. 1(a). This cross slot is etched on either side of the square-shaped substrate ($L_s = W_s = 15.5$ mm) having $\epsilon_r = 2.2$, $tan\delta = 0.0009$ and 1.56 mm thickness. The dimensions of the cross-slot design are such as $L = 13.55$ mm and $W = 2.2$ mm for 10 GHz operating frequency. Here the via diameter (d_r) and the periodicity between the vias (d_p) are kept at 0.7 mm and 1.55 mm respectively to avoid the field leakage. A substrate layer sandwiched between two metallic plates and surrounded by metallic vias makes the SIW structure a metallic cavity, which operates at TM_{mnp} mode, where the resonant frequency can be expressed as [3]

$$f_{TM_{mn0}} = \frac{C_0}{2\sqrt{\epsilon_r}}\sqrt{(m/L_{xeff})^2 + (n/W_{yeff})^2} \quad (1)$$

where $L_{xeff} = L_s - \frac{d_r{}^2}{0.95 d_p}$ and $W_{yeff} = W_s - \frac{d_r{}^2}{0.95 d_p}$

The expressions are valid for $d_p < 0.5\lambda_0\sqrt{\epsilon_r}$ and $d_p < 4d_r$, Where d_p, is selected greater than $2d_r$.

The S-parameter response for the design stage 1 FSS unit cell is provided in Fig. 2. To further improve the bandwidth, the convention cross slot is modified to a novel exponential taper cross slot in design stage 2 as shown in Fig. 1(b). Dimensions of exponentially tapered cross slots are governed by the following equation [15]

$$w(i) = w_1.e^{-\alpha i}, i = x, y \quad (2)$$

Here, $w(i)$ represents the width at position i along the length, w_1 is the initial width at the starting point ($i = 0$), and α is the taper rate or decay constant which determines the rate of change in width along the length. The new SIW-based FSS slot dimensions such as $L_s = W_s = 17$ mm and $L = 15.4$ mm where width varies along the length. The via diameter (d_r) is set to 1.0 mm, and the pitch distance (d_p) between two vias is chosen as 1.7 mm to confine the field within the cavity [1].

Fig. 2 shows the S-parameter response for SIW-based conventional as well as exponentially tapered cross-slots FSS design. The conventional cross slot FSS has a transmission bandwidth of 21.12% (8.68 GHz to 10.73 GHz). On the other hand, the proposed exponential tapered FSS has an improved transmission bandwidth of 33.8% (8.69 GHz to 12.07 GHz). In general, the SIW-based FSS provides a wider passband response compared to its non-SIW counterparts due to the formation of two resonant modes in SIW-FSS such as the resonance generated by the periodicity and the resonance due to the SIW cavity [26]. In addition, the utilization of the exponential tapering for FSS design instead of a conventional square slot provides the enhanced passband response due to the continuous impedance transition corresponding to continuous various of slot width (see Fig. 2(b)) thereby achieving 56% improvement in transmission bandwidth (-3 dB) as shown in Fig. 2(b).

III. PARAMETRIC STUDY

A parametric study is conducted to get a thorough understanding and analyse the performance of the structure. The effect of the tapering factor, via dimensions, polarization and angle of incident wave are presented in detail.

A. Effect of tapering factor, α

The tapering factor α is the main design parameter of the proposed design. The value of α is varied from 0.11 to

[1]Note, here the updated values for L_s, W_s, L, d_p and d_r are chosen to keep the initial passband frequeny of the proposed exponential taper to that of conventional cross slot for a valid comparison.
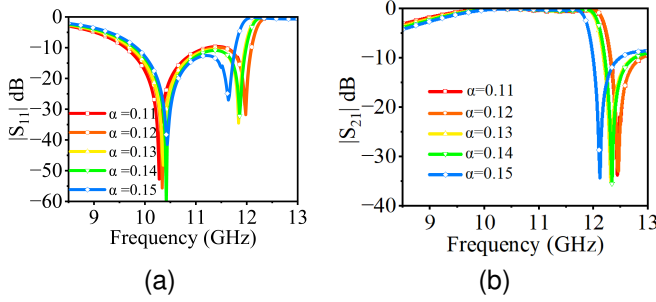
Fig. 3. Effect of variation of tapering factor, 'α' on S-parameters of exponentially tapered cross slot SIW based FSS unit cell (a) Reflection coefficient Vs frequency, and (b) Transmission coefficient Vs frequency.
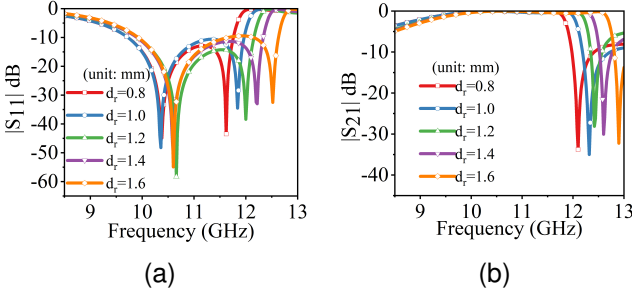

Fig. 5. Effect of incidence angle on S-parameters of exponentially tapered SIW based FSS for TE mode (a) Reflection coefficient Vs frequency, and (b) Transmission coefficient Vs frequency.

Fig. 4. Effect of variation of via diameter, dr on S-parameters of exponentially tapered cross slot SIW based FSS unit cell (a) Reflection coefficient Vs frequency, and (b) Transmission coefficient Vs frequency.

Fig. 6. Effect of incidence angle on S-parameters of exponentially tapered SIW based FSS for TM mode (a) Reflection coefficient Vs frequency, and (b) Transmission coefficient Vs frequency.

0.15, with a step size of 0.01, while keeping the value of $L = 15.4$ mm. The reflection and transmission coefficient versus frequency for various values of α are shown in Fig. 3. It was observed that as α increases, the -3 dB transmission bandwidth decreases. This is due to the smooth transition of the impedance at smaller values of α. Simultaneously, the transmission zero also shifts to the left with increasing α. The tapering factor $\alpha = 0.13$ shows the optimal performance throughout the frequency range and provides 33.8% of fractional bandwidth corresponding to -3 dB transmission coefficient.

B. Effect of via dimensions

As inappropriate dimensions of via can result in leakage, the dimensions of vias have been carefully studied. The diameter of the vias d_r is varied within the range of 0.8 mm to 1.6 mm, with a step size of 0.2 mm. Fig. 4 depicts the reflection and transmission coefficient vs frequency. It is observed that as the radius of via increases, the bandwidth of the unit cell also increases. The transmission coefficient sharp roll-off shifts towards higher frequency with the increase in via diameter. Since the increase in via diameter reduces the gap between adjacent via and may create a physical notch in the structure. Similarly, a smaller via diameter can increase the field leakage. Considering the available fabrication facility, it is decided to maintain the via diameter at 1 mm thereby reducing the field leakage and getting the satisfactory transmission bandwidth as shown in Fig. 4(b).
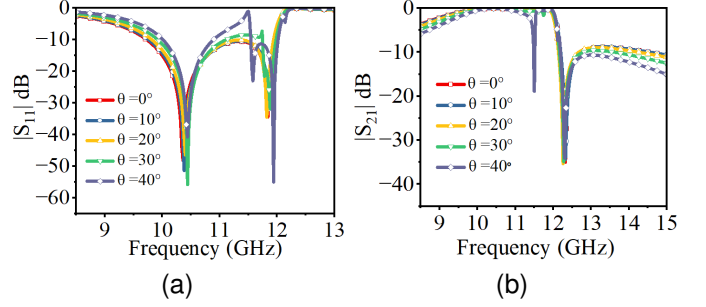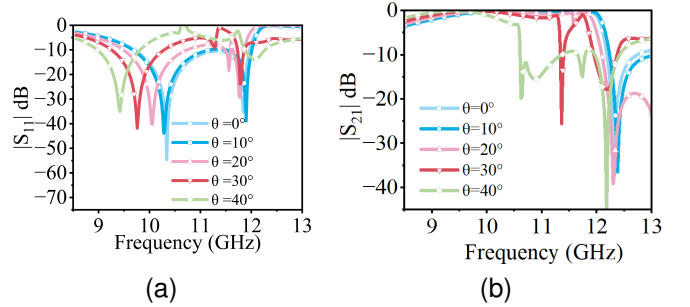
C. Effect of incidence angle

The proposed structure is examined for various incident angles for TE and TM polarization. The behaviour of the structure is analyzed up to an oblique incidence of 40°. The resulting response is shown in Fig. 5 and Fig. 6 for TE and TM polarization respectively. The structure demonstrates a very good flat-top response for oblique incidence angles till 30° for TE polarized waves. However, the structure exhibits an transmission null at 30° for TM polarization, as shown in Fig. 6. The proposed structure maintains a 1 dB (90% transmission) insertion loss up to an incident angle of 30° for TE and 20° for TM polarization. In case of TM mode polarization, the shift of resonance behavior can be observed in Fig. 6.

D. Effect of Tapering factor on Angular stability

The angular study was conducted by maintaining a constant angle of incidence while varying the tapering factor. Fig. 7 shows the effect of variation of α for a constant incidence angle on Reflection characteristics of the proposed structure for TE polarized wave for incident angle, between $\theta = 10°$ and $\theta = 30°$, and the tapering factor, α, between 0.11 and 0.15 This study is conducted to examine the impact of the specific incident angle when the tapering factor is altered. When the tapering factor was varied, an enhancement in bandwidth was observed. It is observed that adjusting the tapering factor allows for flexibility in the design to achieve varying bandwidths.
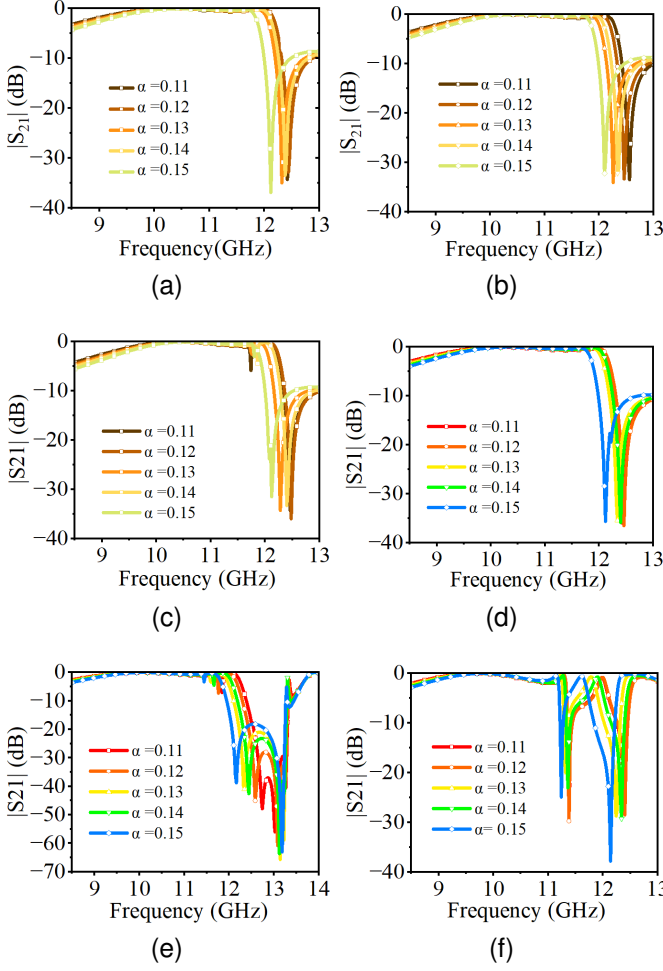
(a) (b) (c) (d) (e) (f)

Fig. 7. Variation of transmission coefficient with frequency (TE Polarisation) (a) theta= $\theta = 10°$ (b) $\theta = 20°$ (c) $\theta = 30°$. (TM Polarisation) (d) $\theta = 10°$ (e) $\theta = 20°$ (f) $\theta = 30°$

Fig. 8. (a)The proposed exponentially tapered SIW based FSS unit cell structure using FR4 substrate, (b) S-Parameters of the proposed exponentially tapered slot SIW based FSS unit cell

TABLE I
COMPARISON OF TRANSMISSION BANDWIDTH OF RT DUROID AND FR4

Type of design	RT Duroid BW (GHz)	FBW	FR4 BW (GHz)	FBW
Traditional Cross Slot	8.68 to 10.73	21.12%	9.29 to 11.10	18.1%
Exponential Tapered Slot	8.69 to 12.07	33.8%	8.96 to 11.79	28.3%

BW: -3 dB transmission Bandwidth, FBW: Fractional Bandwidth

Fig. 9. Prototype of fabricated exponentially tapered SIW based FSS.

IV. FABRICATION AND MEASUREMENT

The structure proposed and studied in earlier sections is designed using Rogers's RT Duroid. To investigate the scalability of the design concerning the substrate material and to get a low-cost prototype development followed by design validation, the same structure is re-designed and studied using FR4 substrate having 1.56 mm thickness as shown in Fig. 8(a). The design dimensions of the proposed exponential taper slot are tuned to make the structure operate within the X-band. Hence, the corresponding unit cell dimensions such as L = 11.6 mm, $L_s = W_s = 12.5mm$, $d_r = 0.6$ mm, and $d_p = 1.25$ mm. The corresponding S-parameter response is shown in Fig. 8(b). The transmission bandwidth of the design is 2.83 GHz (8.96 GHz to 11.79 GHz, i.e., 28.3%). Fig. 9 shows the prototype of fabricated exponentially tapered SIW based FSS. A comparative study of the FSS design using RT Duroid and FR4 substrate is provided in Table I. It shows that the proposed exponential taper SIW-FSS compared to the conventional design exhibits $\approx 55\%$ bandwidth improvement for both substrates.

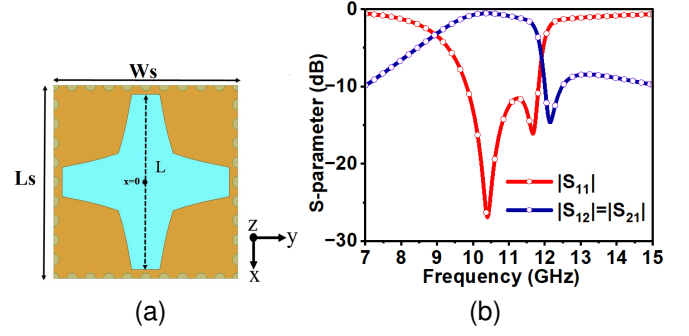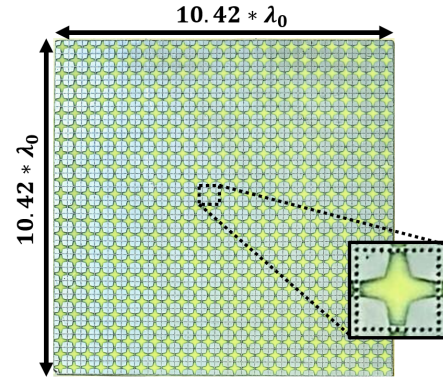The experimental setup has been shown in Fig. 10. The dimensions of the fabricated square-shaped SIW-based expo-

nential taper FSS are $312.5 \times 312.5 mm^2$ which is $10.42\lambda_0$.The measurement setup includes two standard high gain horn antennas connected to a Vector Network Analyzer (VNA), where FSS under test is placed in between the antennas. Initially, the FSS is excited with a plane wave incident normally using the transmitting horn antenna(Tx) placed at a far-field distance. Then, the received power is observed through the receiver horn antenna (Rx) connected to the VNA and the measured transmission coefficient is compared with the simulation as shown in Fig. 11. The measured results are in good agreement with the simulated results with a -3 dB transmission bandwidth of 3.1 GHZ. Table II shows the comparison of the proposed work with the existing literature. The proposed work shows high transmission bandwidth and comparatively low insertion loss.

V. CONFORMAL ANALYSIS

The planar unit cell element has been strategically utilized to achieve a conformal structure by enveloping it around
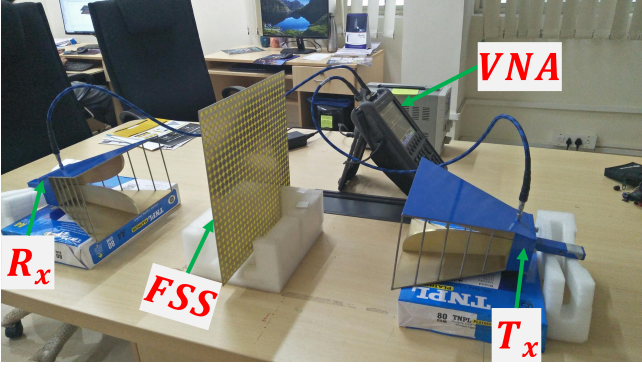
Fig. 10. Experimental setup to measure transmission coefficient of proposed FSS structure. (Tx: Transmitter, Rx: Receiver, VNA: Vector Network Analyzer, FSS: Frequency selective surface under test)
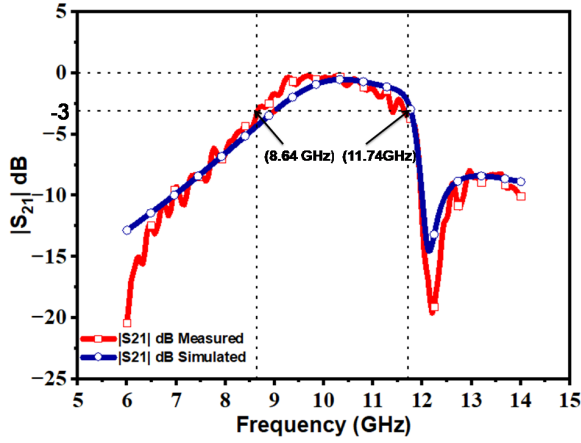

Fig. 12. Conformal analysis of proposed unit cell by wrapping it on a cylindrical surface of radius R_c.

Fig. 11. Comparison of Measured and simulated Transmission Coefficient vs Frequency response of fabricated SIW-based FSS using FR4

Fig. 13. Variation of S parameters with frequency for various values of cylinder radius R_c. (a) Reflection coefficient Vs frequency, and (b) Transmission coefficient Vs frequency.

the cylindrical surface as shown in Fig. 12. This conformal shape introduces variations in the surface area of the unit cell element as perceived by electromagnetic (EM) waves, potentially impacting the performance of the conformal unit cell. To investigate the influence of bending, the performance of the structure has been analyzed at different cylinder radii, denoted as R_c, ranging from 40 mm to 100 mm. The cylindrical bend feature in Ansys HFSS has been employed to accurately model the conformal shape. The analysis focuses on examining the reflection and transmission coefficients to study the effect of bending, as depicted in Fig. 13. The results indicate that the conformal unit cell demonstrates favourable
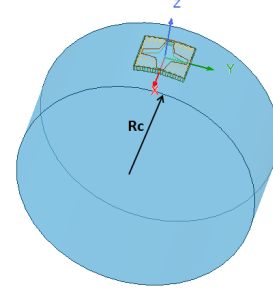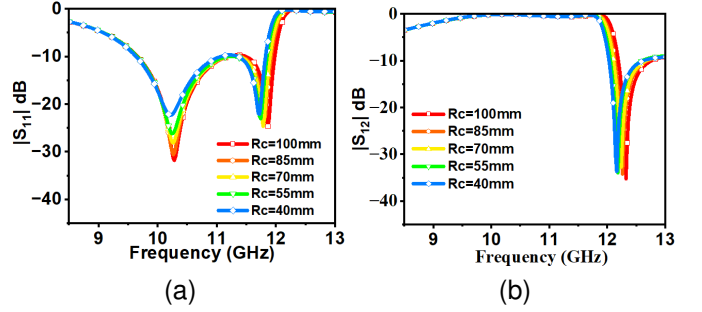
impedance matching and transmission performance within its operating band, even under maximum bending conditions ($R_c = 100$ mm). As the radius of curvature (R_c) decreases, the propagation direction of the electromagnetic waves through the structure doesn't deviate more significantly.

VI. CONCLUSION

A bandpass FSS (Frequency Selective Surface) structure based on SIW (Substrate Integrated Waveguide) is designed using an exponential tapering technique. Compared to the traditional cross-slot-based structure the exponential tapering provides the $\approx 55\%$ improved passband characteristics, low insertion loss and sharp rolloff. The effective use of the tapering factor or decay constant provides flexibility in choosing wider transmission bandwidth or better reflection characteristics. The proposed design provides a wider transmission fractional bandwidth of 33.8% and 28.3% using RT-duroid and FR4 substrate respectively. A low-cost prototype of the design using the FR4 substrate is fabricated and the measured result is compared with the simulated one. The proposed design is suitable for the X-band application.

REFERENCES

[1] B.A.Munk, Frequency selective surfaces: Theory and design, Wiley, New York, 2000.

[2] Guo Qing Luo, Wei Hong, Zhang-Cheng Hao, Bing Liu, Wei Dong Li, Ji Xin Chen, Hou Xing Zhou, Ke Wu, "Theory and Experiment of Novel Frequency Selective Surface Based on Substrate Integrated Waveguide.Technology", *IEEE Transactions on Antennas and Propagation*, Vol.53,No. 12, Dec 2005.

TABLE II
COMPARISON OF THE PROPOSED WORK WITH RECENT LITERATURE.

Ref.	Type of Substrate	Type of Mechanism	FSS Size(λ_0^2)	Insertion Loss(dB)	BW (%)
[3]	RT Duroid	Step tapered cross slot	$5.3\lambda_0 \times 5.3\lambda_0$	0.1	24.9%
[17]	FR-4	Mushroom like cavity	$6.67\lambda_0 \times 6.67\lambda_0$	Not given	12.3%
[18]	RT Duroid	Conical Ogive slot	$5\lambda_0 \times 5 \times \lambda_0$	1	13%
[19]	RT Duroid	Cross slot	Not given	Not given	36.2%
[20]	RT Duroid	Stacked SIW Structure	$5.87\lambda_0 \times 5.97\lambda_0$	0.86	4.5%
[27]	Rogers 4320	DSPSL	$4.625\lambda_0 \times 4.825\lambda_0$	0.86	18.4%
[28]	F4BM-2	Single SIW	$10.77\lambda_0 \times 10.775\lambda_0$	0.44	5.5%
[29]	F4B-2	Composite Structure	$10\lambda_0 \times 10\lambda_0$	0.80	12%
[30]	Not given	Single SIW	Not given	0.7	12.7%
Prop.1	**FR-4**	**Exponentially tapered slot**	$\mathbf{10.42\lambda_0 \times 10.42\lambda_0}$	**0.6**	**31%**

FSS: Frequency selective surface, BW: -3 dB transmission Bandwidth

[3] V. Krushna Kanth and S. Raghavan, "EM Design and Analysis of Frequency Selective Surface Based on Substrate-Integrated Waveguide Technology for Airborne Radome application," in IEEE Transactions on Microwave Theory and Techniques, vol. 67, no. 5, pp. 1727-1739, May 2019.

[4] J. Singh, M. Najim, V. Agarwala, D. Singh and G. D. Varma, "Critical analysis of Frequency Selective Surfaces for dual band GSM-900 1800 MHz transmission," 2015 National Conference on Recent Advances in electronics Computer Engineering (RAECE), Roorkee, India, pp. 207-210,2015.

[5] Yousef Mannaa, Rabah W. Aldhaheri, "New Dual-Band Frequency Selective Surface for GSM Shielding in Secure-Electromanetic Buildings Using Square Loop Fractal Configurations", 16th Mediterranean Microwave Symposium (MMS), 14-16 November 2016.

[6] K. Katoch, N. Jaglan and S. D. Gupta, "A Review on Frequency Selective Surfaces and its Applications," International Conference on Signal Processing and Communication (ICSC), pp. 75-81,2019.

[7] Varikuntla, Krushna kanth Singarav, R. "Review on Design of Frequency Selective Surfaces based on Substrate Integrated Waveguide Technology".Advanced Electromagnetics. 7. 101-110. 10.7716/aem.v7i5.751,2018.

[8] V. K. Kanth and S. Raghavan, "Band-Pass FSS Radome with Sharp Band Edge Characteristics Based on Substrate Integrated Waveguide Technology," IEEE Indian Conference on Antennas and Propagation (InCAP), pp.1-4,2019 , pp.15-64.

[9] R. Mittra, C. H. Chan and T. Cwik, "Techniques for analyzing frequency selective surfaces-a review," in Proceedings of the IEEE, vol. 76, no. 12, pp. 1593-1615, Dec.1988.

[10] Yu Jian Cheng, "Surface Integrated Antennas and Arrays", CR press,2016.

[11] G Sen, M. Midya and S. Ghosh, "Design of a band pass FSS with a sharp transition response based on SIW technology for satellite application," 2021 5th International Conference on Electronics, Materials Engineering & Nano-Technology (IEMENTech), Kolkata,doi:10.1109/IEMENTech53263.2021.9614742,India, 2021, pp. 1-3,

[12] D. S. Chandu, S. Pradhan, and S. S. Karthikeyan, "SIW-based modified slotted array antenna with circular polarization for X, Ku and K band communications," 46th European Microwave Conference (EuMC), pp. 417-420,2016

[13] P.S. M. Yazeen, C. V. Vinisha, S. Vandana, M. Suprava, and R. U. Nair,"Electromagnetic performance analysis of graded dielectric inhomogeneous streamlined airborne radome, *IEEE Transactions on Antennas and Propagation*,,vol. 65, no. 5, pp. 2718–2723, May 2017.

[14] W. Xu, B.Y.Duan, P.Li, and Y.Qiu, "Study on the electromagnetic performance of inhomogeneous radomes for airborne applications—Part I: Characteristics of phase distortion and boresight error, *IEEE Transactions on Antennas and Propagation*,, vol. 65, no. 6, pp. 3162–3174,Jun. 2017

[15] M. Bozzi, A. Georgiadis, and K. Wu, "Review of substrate-integrated waveguide circuits and antennas," IET Microw. Antennas Propag., vol. 5,no. 8, pp. 909–920, Jun. 2011.

[16] Pozar, David M. Microwave Engineering. Hoboken, NJ :Wiley, 2012. APA Pozar, David M. (2012) page 250-253.

[17] T. Zhong, H. Zhang, X.-L. Min, Q. Chen, and G.-C. Wu, "Wideband Frequency Selective Surface with a Sharp Band Edge Based on Mushroom-Like Cavity," Progress In Electromagnetics Research Letters, vol. 62, pp. 105-110, 2016

[18] K. K. Varikuntla and R. S. Velu (2019), 'Design and development of angularly stable and polarisation rotating FSS radome based on substrate-integrated waveguide technology', IET Microwaves, Antennas and Propagation, vol. 13, no. 4, pp. 478-484, 10.1049/iet-map.2018.5386

[19] M. Qu, Y. Feng, J. Su and S. M. A. Shah, "Design of a Single-Layer Frequency Selective Surface for 5G Shielding," in IEEE Microwave and Wireless Components Letters, vol. 31, no. 3, pp. 249-252, March 2021.

[20] G.W. Chen et al, "High Roll-Off Frequency Selective Surface With Quasi-Elliptic Bandpass Response," in *IEEE Transactions on Antennas and Propagation*, vol. 69, no. 9, pp. 5740-5749, Sept. 2021.

[21] S. Narayan, G. Gulati, B. Sangeetha, and R. U. Nair, "Novel metamaterial-element-based FSS for airborne radome applications, *IEEE Transactions on Antennas and Propagation*,, vol. 66, no. 9, pp. 4695–4707, Sep. 2018.

[22] R. Shavit, Radome Electromagnetic Theory and Design. Hoboken,NJ, USA: Wiley, 2018.

[23] Yin, H. Zhang, T. Zhong, and X. Min, "Ultra-miniaturized low-profile angularly-stable frequency selective surface design," IEEE Trans.Electromagn. Compat., vol. 61, no. 4, pp. 1234–1238, Aug. 2019.

[24] M. W. Niaz, Y. Yin, and J. Chen, "Synthesis of ultra miniaturized frequency-selective surfaces utilizing 2.5-D tapered meandering lines, *IEEE Transactions on Antennas and Propagation*, vol. 19, no. 1, pp. 163–167,Jan. 2020.

[25] Ma, Y. Liu, G. Wan, and A. Pan, "Angularly stable frequency Selective surface using shifted double-sided screens," *IEEE Transactions on Antennas and Propagation*, vol. 19, no. 7, pp. 1192–1196, Jul. 2020.

[26] G. Q. Luo et al., "Theory and experiment of novel frequency selective surface based on substrate integrated waveguide technology," *IEEE Transactions on Antennas and Propagation*, vol. 53, no. 12, pp. 4035-4043, Dec. 2005.

[27] B. Li and Z. Shen, "Three-Dimensional Dual-Polarized Frequency Selective Structure With Wide Out-of-Band Rejection," in *IEEE Transactions on Antennas and Propagation*, vol. 62, no. 1, pp. 130-137, Jan. 2014.

[28] Wang, Xian, Zhou, Dongfang , Wang, Yue , Liu, Qikun, An, Na. (2021). Design of high roll-off frequency selective surface based on single-layer SIW cavity with fully canonical filtering responses. Electronics Letters.

[29] Liu, N., Sheng, X., Zhang, C., Guo, D. (2019). Design and Synthesis of Band-Pass Frequency Selective Surface with Wideband Rejection and Fast Roll-Off Characteristics for Radome Applications. *IEEE Transactions on Antennas and Propagation*, 1–1.

[30] Yang, Linchuan , Zhou, Dongfang , Zhang, Dewei , Wang, Xian ,Qian, Hang. (2023). Design of a High-Selectivity Frequency Selective Surface Based on SIW Technology. 1-3.